Nanoscale

www.rsc.org/nanoscale

Volume 3 | Number 3 | March 2011 | Pages 753–1276

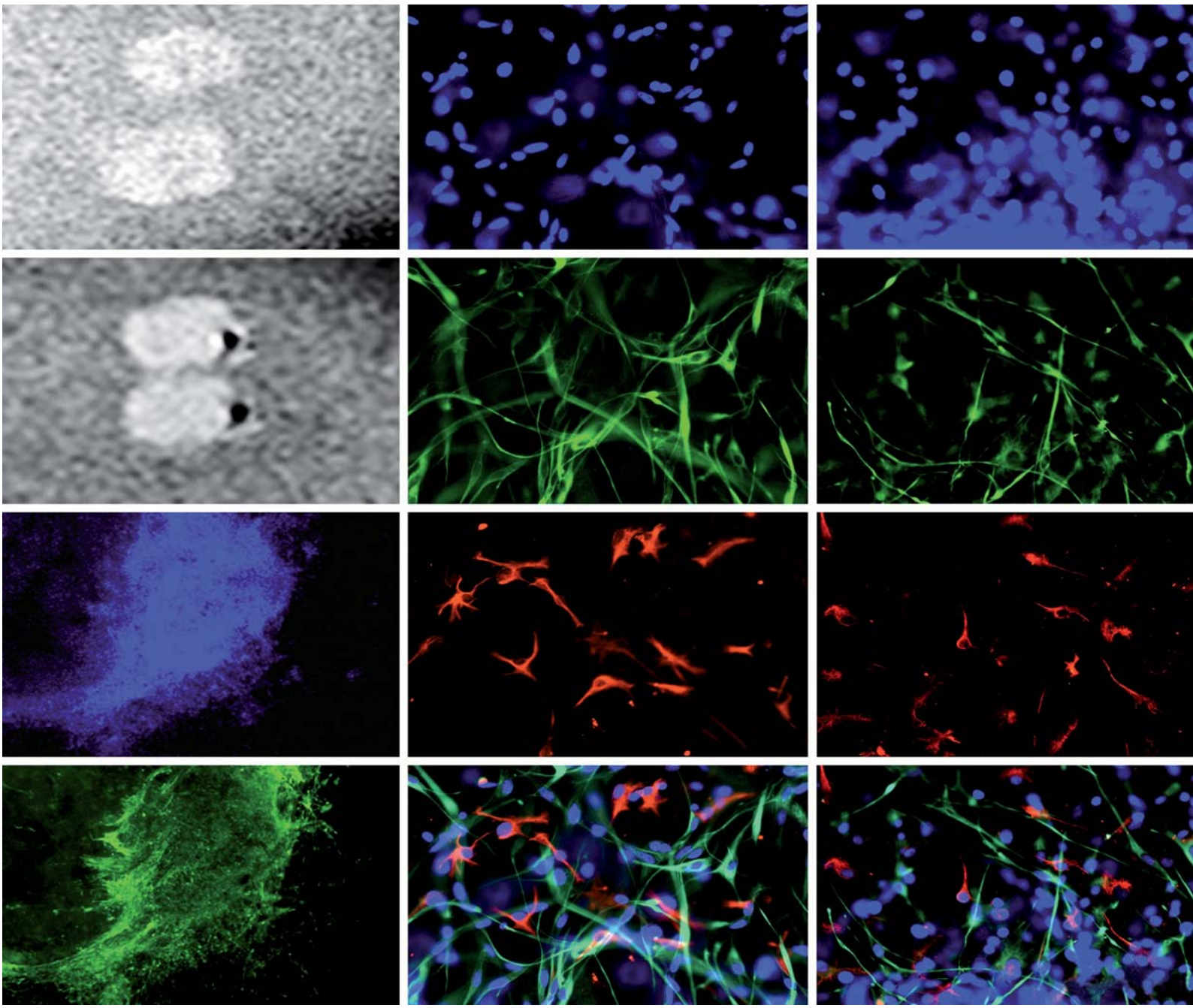

ISSN 2040-3364

COVER ARTICLE
Thanh *et al.*
Magnetic CoPt nanoparticles as MRI contrast agent for transplanted neural stem cells detection

HOT ARTICLE
Lee *et al.*
Small-sized silicon nanoparticles: new nanolights and nanocatalysts

RSC Publishing

2040-3364(2011)3:3;1-P

Nanoscale

Dynamic Article Links

Cite this: DOI: 10.1039/c0nr00846j

www.rsc.org/nanoscale

PAPER

Magnetic CoPt nanoparticles as MRI contrast agent for transplanted neural stem cells detection

Xiaoting Meng,[a] Hugh C. Seton,[b] Le T. Lu,[c] Ian A. Prior,[d] Nguyen T. K. Thanh*[ef] and Bing Song*[ab]

Received 9th November 2010, Accepted 6th December 2010
DOI: 10.1039/c0nr00846j

Neural stem cells (NSCs) exhibit features that make them suitable candidates for stem cell replacement therapy and spinal cord reconstruction. Magnetic resonance imaging (MRI) offers the potential to track cells *in vivo* using innovative approaches to cell labeling and image acquisition. In this study, experiments were carried out to optimize the loading condition of magnetic CoPt hollow nanoparticles (CoPt NPs) into neural stem cells and to define appropriate MRI parameters. Both cell viability and multipotency analysis showed that CoPt NPs at a concentration of 16 μg ml^{-1} reduced T_2 relaxation times in labeled rat NSCs, producing greater contrast on spin echo acquisitions at 4.7 T, yet did not affect cell viability and *in vitro* differentiation potential compared to controls. After optimizing nanoparticle loading concentrations and labeled cell numbers for MRI detection, CoPt-loaded NSCs were transplanted into organotypic spinal cord slices. The results showed that MRI could efficiently detect low numbers of CoPt-labeled NSCs with the enhanced image contrast. Our study demonstrated that MRI of grafted NSCs labeled with CoPt NPs is a useful tool to evaluate organotypic spinal cord slice models and has potential applications in other biological systems.

1 Introduction

Currently, there is intense interest in NSC transplantation as a possible method of repairing spinal cord injury.[1–3] MRI is a noninvasive technique which has been used to track transplanted cells labeled with super-paramagnetic nanoparticles as contrast agents, in longitudinal studies on living animals.[4] It has been reported that cobalt (Co) nanoparticles have much higher saturation magnetization values than iron oxide at room temperature, having a greater effect on proton relaxation, leading to improved MR contrast and allowing smaller particle cores to be used without compromising sensitivity.[5] Superparamagnetic iron oxide nanoparticles (NPs) have been used as contrast agent for magnetic resonance imaging (MRI).[6] In particular, several studies have applied magnetic iron oxide NPs to track NSCs *in vivo*.[7,8] However, they suffer from low magnetic moment, therefore, high concentration of NPs or bigger size NPs is needed.[5] We have successfully used high magnetic moment Co NPs as a contrast agent, but they lack long-term stability (more than few months).[9] We have developed CoPt hollow NPs that are stable in a wide range of pH = 1.5–10 and up to 2 M NaCl for many months.[10] Only with this superstability of CoPt NPs, a very extensive study of their interactions with biological cells could be investigated.[10] To date, there has been no report using cells prelabeled with CoPt NPs *in vitro*, the nanoparticle loading for biomedical applications must be optimized for efficient cell labeling without impairing cell survival, proliferation and multipotency, as well as the cellular behaviours during transplantation and integration.[11] Spinal cord slice is a better recipient tissue for transplanted NSCs *ex vivo* because within these cultures the cytoarchitectonic tissue organization is well preserved, and slices can be maintained in culture for longer periods,[12,13] therefore this model closely mimics the *in vivo* environment of stem cell transplantation.

Here we report a simple but efficient *in vitro* protocol to label NSCs with CoPt NPs, and a simple MRI method to visualise the uptake of transplanted CoPt NP-labeled NSCs by spinal cord slices. We optimized both the incubation time and the concentration of CoPt NPs, which allows an efficient labeling of NSCs *in vitro* without impairing their properties. We then used organotypic spinal cord slices that preserve the complete *in vivo* structure of the spinal cord to assess whether *in vivo* imaging of CoPt NP-labeled NSCs will be feasible in future. MRI and histological analysis indicated that it was possible to reliably track 10^6 viable CoPt-labeled NSCs in longitudinal studies.

[a]*School of Dentistry, Cardiff Institute of Tissue Engineering & Repair, Cardiff University, Cardiff, CF14 4XY, UK. E-mail: SongB3@cardiff.ac.uk; Fax: +44 (0)29-20748168; Tel: +44 (0)29-20744182*
[b]*School of Medical Sciences, University of Aberdeen, AB25 2ZD, UK*
[c]*Department of Chemistry, University of Liverpool, L69 3BX, UK*
[d]*Physiological Laboratory, University of Liverpool, Liverpool, L69 3BX, UK*
[e]*The Davy-Faraday Research Laboratory, The Royal Institution of Great Britain, 21 Albemarle Street, London, W1S 4BS, UK. E-mail: ntk.thanh@ucl.ac.uk; Fax: +44 (0)207-670-2920; Tel: +44 (0)207-491-6509*
[f]*Department of Physics & Astronomy, University College London, Gower Street, London, WC1E 6BT, UK*

2 Materials and methods

2.1 Synthesis of CoPt NPs

Two samples containing monodispersed CoPt NPs were prepared by reduction of Co^{2+} and Pt^{4+} simultaneously in water in the presence of the ligands.[10] The morphology and distribution of nanoparticle size were determined by transmission electron microscopy (TEM). Sample 1 was formed by coating CoPt NPs in a mixture of thiolated polyethylene glycol (PEG–SH) and CCALNN peptide (COOH and NH_2 functional groups), producing water disperse nanoparticles with diameters of 10.5 ± 1.5 nm. Sample 2 was formed by coating CoPt NPs with poly(methacrylic acid) pentaerythritol tetrakis(3-mercaptopropionate) (PMAA–PTMP) (COOH functional group) to produce nanoparticles with diameters of 9.5 ± 1.5 nm. Both samples were initially prepared with a CoPt NP concentration of 480 μg ml^{-1} (3 mM), and different concentrations of CoPt NPs in a range from 0.05 mM to 0.5 mM were used for relaxivity measurements and toxicity assays.

2.2 Culturing of neural stem cells

NSCs were cultured from the fetal brain tissue of embryonic day 14 Sprague-Dawley (E14 SD) rats, using the neurosphere method described previously.[14] Briefly, fetal brain tissue was microdissected and mechanically triturated to a single cell suspension and resuspended in serum-free Dulbecco's modified eagle medium (DMEM/F-12 Gibco, UK) containing B27 supplement (Gibco, UK), 20 ng ml^{-1} of human recombinant fibroblast growth factor (FGF-2, Peprotech, London, UK) and 10 ng ml^{-1} of human recombinant epidermal growth factor (EGF) (Peprotech, London, UK). For monolayer growth, neurospheres were digested to single cells using trypsin and EDTA and grown on polyornithine/laminin-coated dishes in DMEM/F-12 medium containing B27 supplement, and FGF-2 and EGF, at 37 °C in 5% CO_2. For transplanted NSCs, cells were incubated in a medium containing 5 μM Hoechst 33342 at 37 °C overnight before cell transplantation takes place.

2.3 Viability analysis of NSCs after CoPt NPs loading

The proliferative activities and viabilities of CoPt-labeled NSCs were evaluated using 48 h and 6 day cell proliferation assays and crystal violet staining, respectively.

NSCs (5×10^4 cells per ml) were grown in a 24 well plate in DMEM/F-12 medium (0.4 ml per well) containing CoPt NPs (Sample 1) at a range of concentrations (2, 4, 8, 16, 24, 40 and 48 μg ml^{-1}) in triplicate. 'CoPt NPs' in the following text refers to Sample 1 if not specified. The cells were collected after 48 h and 6 days respectively and resuspended in 200 μl of DMEM/F-12 medium to allow the cell counting with a haematometer (Superior, Marienfeld, Germany).

Crystal violet is known to stain viable cells that adhere to their culture vessel, giving a linear relationship between the optical density (OD) of crystal violet extracts and cell numbers.[15] We used this method to test the proliferation of CoPt-labeled NSCs, grown and collected in a 24 well plate as above, after 6 days. Before staining, the cells were fixed with 4% formaldehyde for 10–15 min and washed with phosphate buffered saline (PBS). Freshly filtered 0.1% crystal violet was added (200 μl per well) after PBS washing and the wells were incubated at room temperature for 25 min. After washing and aspirating to completely remove the excessive dye, the plates were allowed to dry at room temperature for 10–15 min. 0.5% Triton X-100 was added (0.5 ml per well) and allowed solubilisation of the crystal violet overnight in the dark. The content from the wells were pipetted into a 96 microwell plate for analysis with a VersaMax™ microplate reader (MDS Analytical Technologies, USA) at 595 nm. Two wells without cells were also stained to check for non-specific binding of crystal violet to the surface of the wells.

2.4 TEM analysis of CoPt NP-loaded neural stem cells

NSCs (2×10^6 cells per plate) were grown in the presence of CoPt NPs (16 μg ml^{-1}) in a 35 mm dish for 48 h and then trypsinized and washed with 1.5 ml PBS. Cells were fixed in 2% glutaraldehyde in phosphate buffer overnight at 4 °C. The cells were washed with PBS twice and processed for resin embedding and TEM analysis.

2.5 Organotypic spinal cord slice culture

Organotypic spinal cord cultures were prepared from the thoracic and lumbar spinal cord of Sprague-Dawley 8 day old rat pups as described by Stoppini *et al.*[16] with minor modifications. In brief, the thoracic and lumbar spinal cords were dissected. Subsequently, spinal cords were sliced into 500 μm-thick sections with McIlwain tissue chopper (The Mickle Laboratory Engineering Co. Ltd, UK). The slices were cultured in a Petri dish containing Matrigel (B.D. Biosciences, UK). These Petri dishes with the spinal cord slice were kept in a 5% CO_2 incubator at 37 °C. The medium consists of HEPES buffer (25 mM, Gibco), fetal calf serum (15%, Invitrogen) and DMEM/F-12, and was changed twice weekly.

2.6 Co-culturing CoPt NPs/Hoechst-labeled NSCs within spinal cord slices

We prepared the CoPt NP/Hoechst 33342-labeled NSC suspension at the concentration of 1×10^6 cells per μl. We topically implanted 2 μl of such suspension to the organotypic spinal cord slices, followed by MRI imaging at either 1 day ($n = 6$) or 2 weeks ($n = 3$) after the start of the slice/NSCs co-culture.

2.7 Magnetic resonance imaging

Imaging was carried out with a Surry Medical Imaging Systems (SMIS) scanner, based on a 4.7 T, 300 mm superconducting magnet (Magnex, UK). The relaxivities of CoPt NPs were measured to assess the minimum number of CoPt NP-labeled NSCs detectable by MRI.

The CoPt NPs synthesised in Section 2.1 were deposited in twelve, 8 mm diameter test tubes. These tubes were imaged at 4.7 T using a commercial quadrature birdcage resonator of 110 mm internal diameter (Morris Instruments, Ontario, Canada) to generate radiofrequency (RF) transmit pulses and receive signals. Longitudinal and transverse relaxivities of the solutions were determined at 25 °C from spin echo MRI, with coronal image slices positioned to intersect the liquid in the tubes. Sample

This journal is © The Royal Society of Chemistry 2011

T_2 values were measured by acquiring a spin echo image set with 80 mm field of view (FOV), 128 × 128 pixels, slice thickness 5 mm and 200 kHz bandwidth, with a fixed repetition time (TR) of 2000 ms and echo times (TE) varied between 20 and 500 ms. Mean image intensities, S, were recorded over the image set from regions of interest placed in each test tube. These data were then plotted as a function of TE, T_2 was calculated by fitting the function $S = S_0 e^{-TE/T_2}$ and the transverse relaxivities, r_2, of Samples 1 and 2 were determined from the gradients of straight lines fitted to plots of $1/T_2$ *versus* the concentration. Longitudinal relaxivities, r_1, were determined by a similar procedure, but this time TE was fixed at 15 ms, TR varied between 50 and 2000 ms to give saturation recovery data, and mean signal intensities fitted with the function $S = S_0(1 - e^{-TR/T_1})$, yielding T_1 values which allowed r_1 to be calculated for each sample.

To determine the minimum number of CoPt NP-labeled cells detectable by MRI, CoPt-labeled NSC suspensions were prepared in PBS with different cell numbers. NSCs, at approximately 3×10^6 cells per plate, were grown in 6 cm Petri dishes containing 4 ml medium in duplicate. CoPt NPs were added to one plate at the final concentration of 16 μg ml^{-1} and the cells were incubated at 37 °C for 48 h. The NSC aggregates containing 10^4, 10^5, 1.5×10^6 and 3×10^6 cells were then transferred to eppendorf tubes. Unlabeled cells of 3×10^6 were transferred to another eppendorf tube to act as a control. Cells were fixed using 4% formaldehyde and after the fixative was removed, the tubes were filled with PBS and centrifuged at 1000 rpm min^{-1} in a Heraeus Pico 17 microcentrifuge (ThermoFisher Scientific, Germany) taking care to minimise air bubbles. Multi-echo-multi-slice (MEMS) MRI was used to image sagittal sections through the eppendorf tubes with 40 mm FOV, 256 × 256 pixels, 2 mm slice thickness, 100 kHz bandwidth, TR 2000 ms, a base echo time TE of 18 ms and 16 echos.

To investigate the potential of MRI to detect grafted cells, 2×10^6 CoPt NP-labeled NSCs were implanted to nine, 500 μm-thick spinal cord slices with a micropipette. MR images were obtained from CoPt NP-labeled NSCs containing spinal cord slices at one day or two weeks after transplantation. To improve the signal to noise ratio of these images, the dish was placed directly above an in-house designed, 20 mm diameter, single turn, receive-only surface coil, with transmit pulses generated by the birdcage resonator. Spin echo MRI acquisitions used a 25 mm FOV, 256 × 256 pixels, 0.5 mm image slice (coplanar with the spine slices), 20 kHz bandwidth and TR 2000 ms/TE 30 ms.

2.8 Immunofluorescent analysis

NSCs and spinal cord slices were fixed with 4% paraformaldehyde for 20 min, permeabilized with 0.2% Triton X-100 for 10 min and incubated in blocking solution (1% BSA in PBS) for 10–30 min, followed by incubation with primary antibodies at 4 °C overnight. After extensive washing with the blocking solution, cells were incubated with secondary antibodies at 37 °C for 1 h. Then, NSCs and spinal cord slices were mounted in Vectashield mounting medium with or without DAPI (Vector Laboratories, Peterborough, UK) respectively. All antibodies were diluted in blocking solution. The primary antibodies used were mouse monoclonal anti-nestin (1 : 200), mouse/rabbit anti-Tuj1 (1 : 100) and rabbit anti-GFAP antibodies (1 : 100; Abcam, Cambridge, UK). The secondary antibodies were FITC conjugated goat anti-mouse and anti-mouse/rabbit IgGs, and TRITC conjugated goat anti-rabbit IgG (1 : 200; Jackson ImmunoResearch, UK).

To determine the percentage of the nestin/Tuj1/GFAP positive cells, the numbers of Hoechst/DAPI-labeled cell nuclei and those double-labeled with FITC/TRITC were counted. NSCs and slices were observed and recorded with a fluorescence microscope (E400 ECLIPSE, Nikon, Japan). Nestin/Tuj1/GFAP expression was qualified and quantified using random sampling (3 visual fields per slice, $n = 3$).

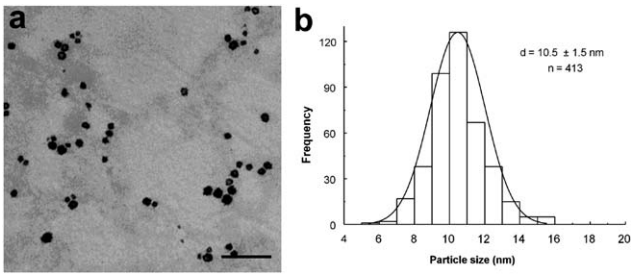

Fig. 1 Morphology and dimension distribution of CoPt nanoparticles. (a) TEM image of CoPt hollow nanoparticles synthesised in the presence of 0.24 mM PEG–SH and 0.12 mM CCALNN (Sample 1). (b) Distribution histogram of CoPt nanoparticle dimension. Bar: 50 nm in (a).

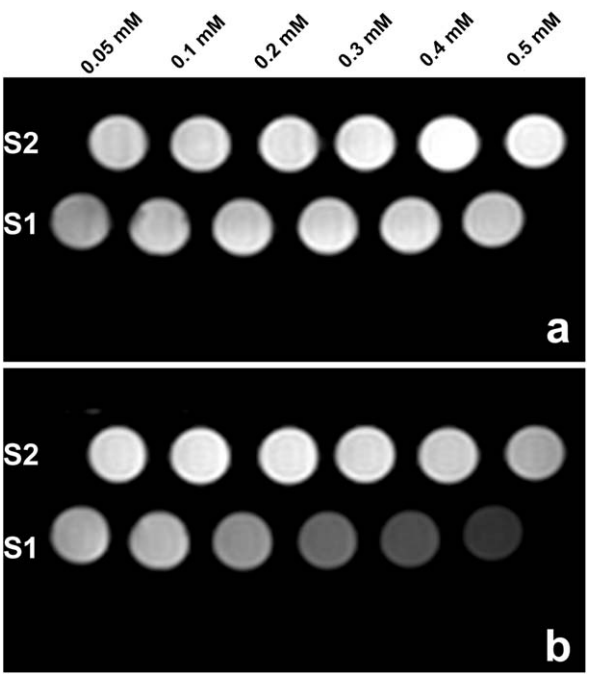

Fig. 2 Dependence of MR relaxation on nanoparticle concentration. (a) A set of six saturation recovery spin echo images (TR 50–2000 ms/TE 15 ms) used to determine T_1 at 4.7 T. From left to right: CoPt nanoparticle concentrations of 0.05 mM (8 μg ml^{-1}), 0.1 mM (16 μg ml^{-1}), 0.2 mM (32 μg ml^{-1}), 0.3 mM (48 μg ml^{-1}), 0.4 mM (64 μg ml^{-1}) and 0.5 mM (80 μg ml^{-1}). (b) A set of six fully recovered spin echo images (TR 2000 ms/TE 20–500 ms) used to determine T_2. In each image the upper row represents Sample 2 (9.5 ± 1.5 nm) and the lower row represents Sample 1 (10.5 ± 1.5 nm).

2.9 Apoptosis detection

Apoptosis was analyzed using TUNEL apoptosis detection kit (Millipore, UK) following the manufacturer's instructions. Cells were counterstained with 5 μM Hochest 33342. Unpaired Student's *t*-test (two-sample assuming unequal variances) was used for statistical analysis.

3 Results and discussion

Neurotransplantation holds great promise for the treatment of acute and chronic central nervous system diseases.[3] Noninvasive cellular imaging allows the real-time tracking of grafted cells as well as the monitoring of their migration. MRI, with its high spatial resolution, is the ideal modality for *in vivo* cell tracking.[4] Tagging cells with nanoparticles has been shown to induce sufficient MR cell contrast for *in vivo* imaging of neural cell migration.[11,17] Before CoPt NP-labeled NSCs can be considered for clinical application, further analysis on the biological effects of CoPt NPs to NSCs is needed. This study describes the development of a simple *in vitro* protocol to label NSCs using CoPt NPs at optimized low dosages that maintain functional properties without acute and delayed toxicity. The new method demonstrates the feasibility of reliable, noninvasive imaging of labeled cells after transplantation into spinal cord slices.

3.1 Optimised CoPt particle concentration and relaxivities at 4.7 T

We prepared two samples of CoPt hollow nanoparticles with different diameters. The MRI detection threshold depends on the CoPt NP concentration per cell, the MRI field strength, RF coil design and pulse sequence parameters all of which affect the SNR (signal to noise ratio).[4,11] The TEM image (Fig. 1a) showed that CoPt NPs (Sample 1) were monodispersed with the mean particle sizes of 10.5 ± 1.5 nm and with narrow size distributions (Fig. 1b). Fig. 2a and b show example spin echo images from the two sets of six tubes of Co NPs dispersed in PBS used to

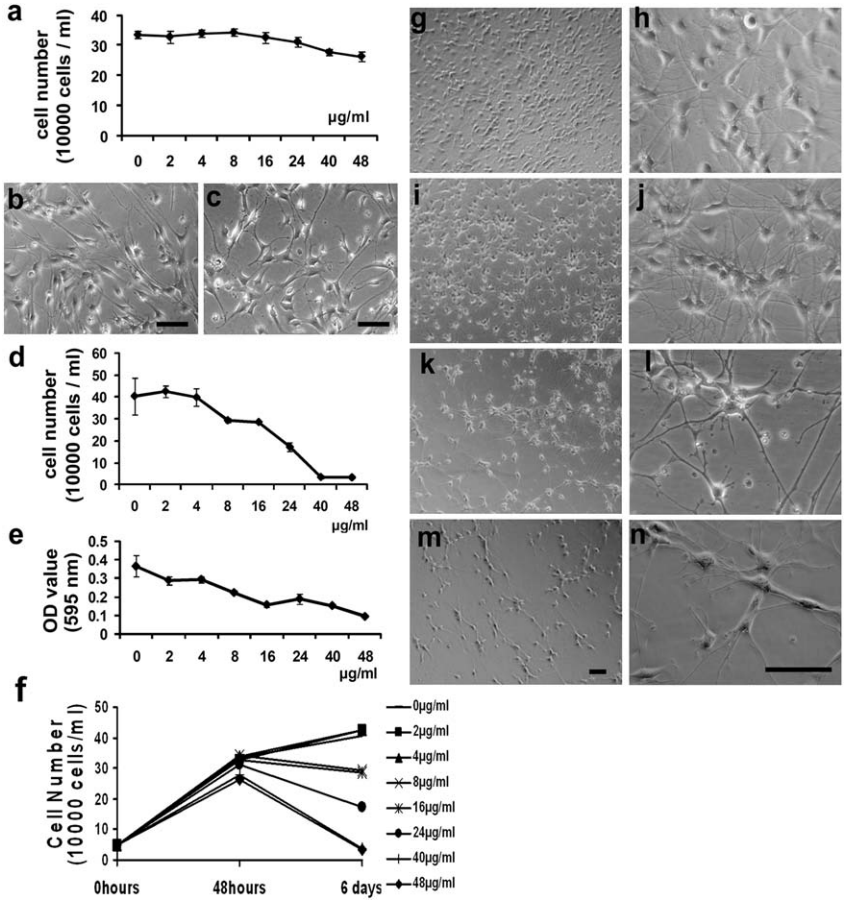

Fig. 3 Cell proliferation and viability after labeling with CoPt nanoparticles. (a) Nanoparticle incubation of 48 h did not affect NSCs survival and proliferation, although the cell numbers decreased slightly when incubated with 40 and 48 μg ml^{-1} of CoPt NPs. (b) Unlabeled NSCs as control. (c) NSCs incubated in 48 μg ml^{-1} CoPt NPs containing medium for 48 h. Under these conditions, CoPt-labeled NSCs did not exhibit morphological difference from unlabeled cells. (d and e) NSCs cell counting and crystal violet staining at day 6 of exposure to CoPt NPs containing medium, respectively. (f) Shows cell growth curve which represents NSCs exposed to different concentration of CoPt NPs at 3 time points. A decrease in the cell counting was observed when exposed to 8 μg ml^{-1} CoPt NPs and above. In comparison with non-labeled NSCs (g and h), no morphological changes were noticed on NSCs labeled with CoPt NP concentration as high as 24 μg ml^{-1} (i and j). When NSCs were exposed to the highest concentration (k and l: 40 μg ml^{-1}; m and n: 48 μg ml^{-1}) and the longest incubation times (6 days), a significant decrease in the cell count was observed in both cell counting and crystal staining, together with significant morphological changes. Bars = 10 μm.

This journal is © The Royal Society of Chemistry 2011

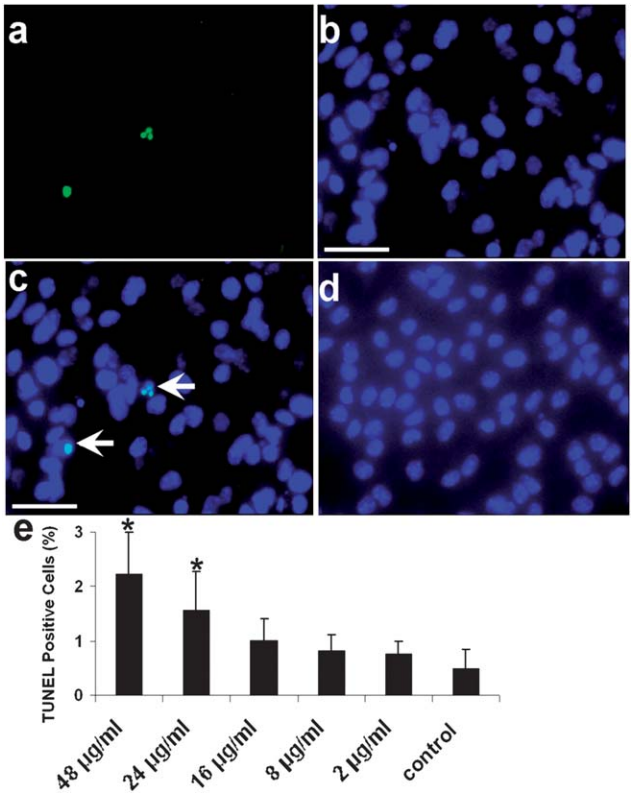

Fig. 4 Apoptosis assay after 6 days incubation with CoPt NPs. Apoptotic cells were detected as FITC-positive cells in TUNEL staining (a), (b) shows nuclei counter staining of Hoechst 33342 and (c) is the merged image of (a) and (b). Shrunk and fragmented nuclei (arrows) were observed after 6 days treatment with CoPt NPs (c) compared to control cells (d). Apoptotic cells were quantified, showing 0.5 ± 0.34%, 1.57 ± 0.71% and 2.24 ± 0.75% TUNEL positive cells in 0, 24 and 48 μg ml^{-1} NP-treated cells respectively (e). *P < 0.05, n = 16 per group. Bars = 10 μm.

determine T_1 (TR 50–2000 ms/TE 15 ms) and T_2 (TR 2000 ms/TE 20–500 ms), respectively. In each image the upper row shows tubes containing Sample 2 (9.5 ± 1.5 nm CoPt NPs) and the lower row shows Sample 1, S1, (10.5 ± 1.5 nm CoPt NPs). Analysis of image data yielded transverse and longitudinal relaxivities, r_2 and r_1, of 38 s^{-1} mM^{-1} and 0.51 s^{-1} mM^{-1} for Sample 1 and 9.3 s^{-1} mM^{-1} and 0.37 s^{-1} mM^{-1} for Sample 2. The results showed that Sample 1 has higher relaxivities than Sample 2 and more suitable for detection at 4.7 T. CoPt NPs are hollow structures consisting of aggregations of small solid nanoparticles. Sample 1 was synthesised in the presence of longer ligand (PEG–SH, 5000 g mol^{-1}), while Sample 2 was prepared using shorter ligand (PMAA–PMTP, 2000 g mol^{-1}).[10] In the presence of longer ligands, bigger solid NPs would form, consequently giving rise to lower relaxivities, which is consistent with our previous finding for the Co NPs system.[7] Longitudinal relaxivities r_1 were increased when the size of Co NPs increased from 3.3 to 3.9 nm.[5] Furthermore the high transverse relaxivity of Sample 1 indicates that T_2-weighted MRI will be the most sensitive technique for detecting NSCs labeled with this type of nanoparticle.

3.2 Cell proliferation and properties after labeling with CoPt nanoparticles

We demonstrated an efficient and non-toxic *in vitro* uptake of Sample 1 CoPt NPs by NSCs. High concentrations (40 and 48 μg ml^{-1}) of CoPt NP labeling only slightly affected NSC proliferation after 48 h incubation. No influence was detectable on cell viability and proliferation at lower concentrations of CoPt NP labeling (2 to 16 μg ml^{-1}). It is known that intracellular free iron overload eventually results in functional impairment and cell death.[6,9,18] In our culture conditions, this delayed toxicity was observed for long-time, up to 6 days, CoPt NP labeling, especially at high concentration of CoPt NP cultivation (24 to 48 μg ml^{-1}).

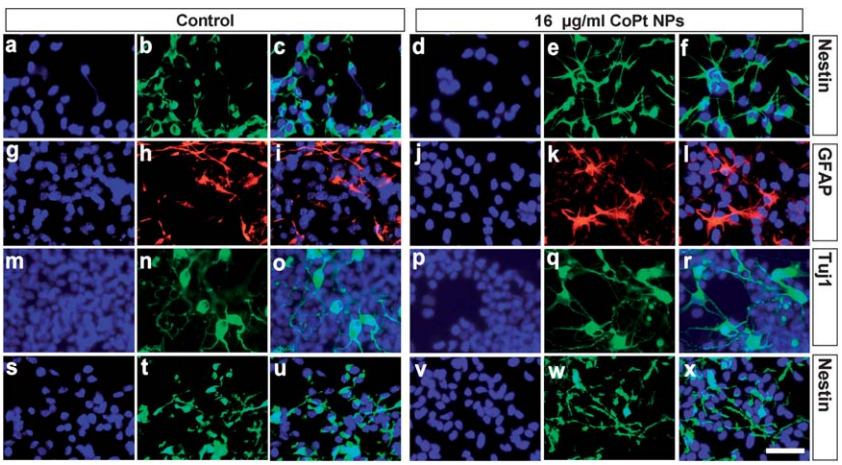

Fig. 5 Optimized CoPt NPs loading does not affect the multipotency of NSCs. A similar proportion of nestin (green) positive cells were observed in CoPt-labeled NSCs 48 h after 16 μg ml^{-1} CoPt NPs incubation (d–f) when compared to unlabeled cells (a–c). Mitogen withdrawal initiated a program of NSCs differentiation. No significant difference was observed between unlabeled (g–i and m–o) and CoPt-labeled NSCs (j–l and p–r) in response to neuronal (m–r, Tuj1 in green) and glial (g–l, GFAP in red) differentiation *in vitro* at day 6 after initiation of differentiation. Similar nestin expression was recorded between unlabeled (s–u) and CoPt-labeled NSCs (v–x). Bars = 10 μm.

Table 1 The percentage of nestin/Tuj1/GFAP positive cells in different groups before and during NSCs differentiation ($n = 5$, mean ± SEM)

	Pre-differentiation	Differentiation (day 6)		
	% of nestin positive cells (48 h)	% of nestin positive cells	% of Tuj1 positive cells	% of GFAP positive cells
Non-labeled NSCs	89.1 ± 1.2	62.8 ± 2.7	12.8 ± 1.1	17.0 ± 2.9
NSCs labeled with 16 μg ml^{-1} CoPt NPs	89.5 ± 0.8	63.8 ± 3.7	11.1 ± 0.7	17.2 ± 4.2

3.2.1 Proliferation of CoPt-labeled NSCs. NSCs (5×10^4 cells per ml) were grown in 24 well plates in EGF/FGF media containing various concentrations of CoPt NPs (from 2 μg ml^{-1} to 48 μg ml^{-1}, 0.4 ml per well) for 48 h and 6 days. Cell counting showed that labeling of NSCs grown as monolayers with Sample 1 for 48 h did not visibly affect survival and proliferation, although there was a slight decrease at nanoparticle concentrations of 40 μg ml^{-1} and 48 μg ml^{-1} (Fig. 3a and f). Under these conditions, CoPt NP-labeled monolayer NSCs did not exhibit morphological differences from unlabeled cells (Fig. 3b and c). When CoPt NP-labeled NSCs were cultured for 6 days, however, a decrease in cell count was observed at a nanoparticle concentration of 8 μg ml^{-1} (Fig. 3d and e), but no change in morphology was observed (Fig. 3h and j). Exposure to the highest concentrations of 40 μg ml^{-1} and 48 μg ml^{-1} and the longest incubation times of 6 days resulted in a significant decrease in both cell counting (Fig. 3d–f), and crystal violet staining and obvious morphological changes (Fig. 3k–n). Therefore we adopted an optimised labeling protocol in which NSCs were exposed to 8 μg ml^{-1} and 16 μg ml^{-1} CoPt NPs for 48 h.

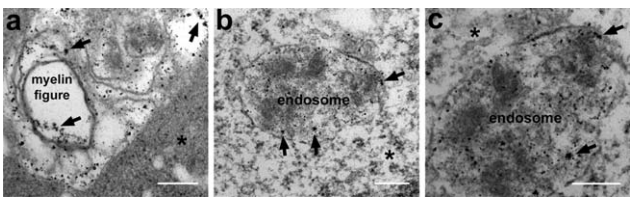

Fig. 6 TEM analysis for nanoparticle-loaded NSCs. The TEM analysis of the NSCs labeled with CoPt NPs showed numbers of CoPt NPs (arrows) present within various compartments of NSCs, including cytoplasm, myelin figure (a) and phago-endosome (b and c). Bars: 200 nm. *: Cytoplasm.

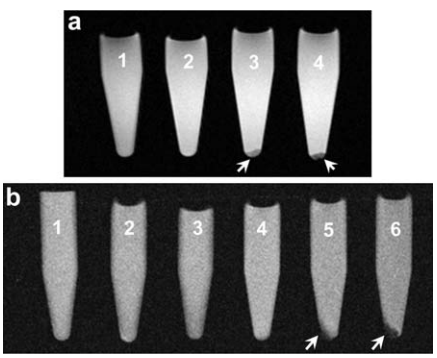

Fig. 7 Optimizing MRI signals of CoPt NP-loaded NSCs. (a) Shows typical T_2-weighted spin echo (TR 1000 ms/TE 18 ms) images of CoPt-labeled NSCs in PBS. a1–a4: PBS only, unlabeled NSCs, 8 μg ml^{-1} and 16 μg ml^{-1} CoPt NPs-labeled NSCs, respectively. (b) Multi-echo acquisition shows hypointense signal regions (arrows) from 16 μg ml^{-1} CoPt-labeled cells in PBS, and the signal was only detectable in the tubes containing 1.5×10^6 or 3×10^6 CoPt-labeled NSCs. b1–b6: PBS only, unlabeled NSCs, 1×10^4, 1×10^5, 1.5×10^6 and 3×10^6 CoPt-labeled NSCs, respectively. Arrows indicate hypointense signal.

3.2.2 Short term treatment with nanoparticles did not trigger cell apoptosis. Apoptosis analysis with TUNEL showed that CoPt NPs did not trigger cell apoptosis after 48 h of treatment with nanoparticles, even at the highest concentration of 48 μg ml^{-1} CoPt NPs (data not shown). In contrast, CoPt NPs incubation for 6 days at both 24 and 48 μg ml^{-1} induced apoptosis of NSCs (1.57 ± 0.71% and 2.24 ± 0.75% TUNEL positive cells, respectively), compared to control cells (with 0.5 ± 0.34% TUNEL positive cells) (Fig. 4a–e; $P < 0.05$, Student's t-test). CoPt NPs incubation at 16 μg ml^{-1} or lower for 6 days did not trigger apoptosis of the cells (data not shown), therefore we chose 16 μg ml^{-1} as the incubation concentration for the rest of the experiments below.

3.2.3 Labeling with CoPt NPs at the optimum concentration does not affect the nestin expression properties and multipotency of NSCs. To confirm that CoPt-labeled NSCs maintain their function *in vitro*, the expression of neuronal progenitor specific marker and cell differentiation capacity were investigated. A similar proportion of nestin positive cells were observed in the 16 μg ml^{-1} CoPt-labeled NSCs (Fig. 5d–f) when compared to the unlabeled control cells, as shown by double immunofluorescence staining in Fig. 5a–c. Moreover, CoPt-labeled NSCs still undergo neural and astrocyte differentiation. There was no significant difference between unlabeled (Fig. 5g–i and m–o) and 16 μg ml^{-1} CoPt-labeled NSCs (Fig. 5j–l and p–r) in response to the neuronal differentiation indicated by Tuj1 expression (Fig. 5m–r) and glial differentiation *in vitro* indicated by GFAP expression (Fig. 5g–l), respectively. There is still a population of nestin positive cells remaining after 6 days of differentiation (Fig. 5s–x). We conclude here that the addition of CoPt NPs at a concentration of 16 μg ml^{-1} did not affect the properties of both proliferation and multipotency of NSCs (Fig. 5g–x; Table 1).

As a result, a 48 h incubation with CoPt NPs at 16 μg ml^{-1} was chosen as the best trade-off in terms of maintaining normal cell properties while resulting in a robust CoPt NP uptake.

3.2.4 TEM analysis of nanoparticle-loaded NSCs. The efficiency and mechanisms of nanoparticle uptake depend on the particle size, cell type, and species specificity.[6,10,19] To confirm

whether nanoparticles entered into NSCs at the labeling efficiency concentration and to localize nanoparticles within the NSCs, cells were grown in the presence of CoPt NPs (16 μg ml^{-1}) for 48 h. TEM analysis, shown in Fig. 6, reveals that a number of CoPt NPs are present within various compartments of NSCs, including the cytoplasm, myelin figure (Fig. 6a) and phagoendosome (Fig. 6b and c). Particles seem to be present mostly in the endosomes and myelin figures, indicating that following uptake by the cells these particles will remain confined within the endocytic system, and we assume this spontaneous endocytosis is due to the relatively small core diameter.

3.3 MRI analysis for nanoparticle-loaded NSCs

Fig. 7a shows an image from a multi-echo acquisition of eppendorf tubes containing NSCs labeled with CoPt NPs at concentrations of 8 μg ml^{-1} and 16 μg ml^{-1} in PBS, together with controls containing PBS only or unlabeled cells in PBS. The transverse relaxation times measured in the liquid above the cells were: 1060 ms (PBS no cells), 680 ms (unlabeled cells), 620 ms (8 μg ml^{-1} labeled cells) and 630 ms (16 μg ml^{-1} labeled cells). The transverse relaxation times measured in the cells at the tip of eppendorf tubes were: 570 ms (PBS no cells), 150 ms (unlabeled cells), 50 ms (8 μg ml^{-1} labeled cells) and 30 ms (16 μg ml^{-1} labeled cells). As expected, those NSCs labeled at the higher concentration showed the lowest T_2. To identify the minimum number of labeled cells required to generate detectable MRI signals, different numbers of NSC samples containing between 10^4 and 3×10^6 cells were imaged after 48 h of 16 μg ml^{-1} CoPt NPs labeling. Fig. 7b shows the multi-echo acquisition which displays a good correlation between numbers of labeled cells and numbers of hypointense pixel output (Fig. 7b3–6). No hypointense signal readout was detectable from unlabeled cells (Fig. 7b2). These results show that T_2-weighted MRI is effective in detecting CoPt-labeled NSCs at as low as 10^6 cells, and that the increase of signal intensity is correlated with the number of labeled cells.

3.4 CoPt-labeled NSCs can be detected by MRI after transplantation into organotypic spinal cord slices

We established organotypic spinal cord slice culture as an *ex vivo* model to address whether CoPt-labeled cells can be detected by MRI after transplantation into the spinal cord. Spinal cord slices were detected as bright elliptic regions under MR scanner (Fig. 8a and b). CoPt-labeled NSCs were grafted into spinal cord slices and represented by dark spots as indicated by arrowheads in the spinal cord slices (Fig. 8b). The Hoechst 33342-labeled cells in Fig. 8c which showed blue fluorescent nuclei under microscope were exactly the same cell population as the dark spots representing cells under MR scanner in Fig. 8b. Fig. 8a shows a typical spin echo MRI image of spinal cord slices that displays regions of hypointense signal attributable to CoPt-labeled cells, which was later confirmed by Hoechst 33342 labeling and anti-nestin immuohistochemical staining immediately after the MRI procedure (Fig. 8c and d). No hypointense MRI signal was detected when similar numbers of unlabeled cells were transplanted (Fig. 8a). The CoPt-labeled NSCs maintained multipotency at 2 weeks after they were transplanted into organotypic spinal cord slices, with evidence to differentiate into astrocytes (Fig. 8g and k) and neurons (Fig. 8j), along with a population of cells that still maintained nestin positive (Fig. 8f).

MRI studies of isolated spinal cord slices showed that low numbers of CoPt NP-loaded NSCs (~10^6 cells) could be detected after 2 weeks following transplantation, and later histological study confirmed the locations of labeled cells. Immunohistochemical staining further confirmed that the CoPt-labeled NSCs show multipotency after being transplanted into spinal cord

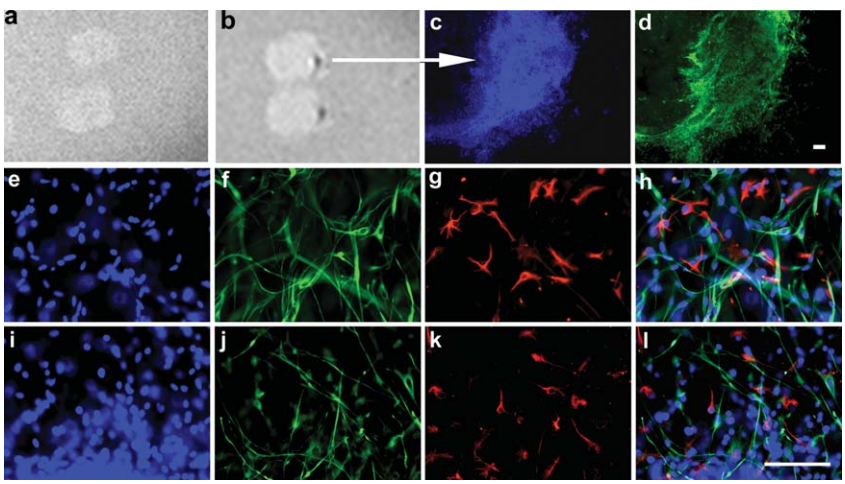

Fig. 8 CoPt-labeled NSCs were detected by MRI and maintained multipotency after transplantation into spinal cord slices. Two spinal cord slices were recorded simultaneously under MR scanner as two bright elliptic regions adjacent to each other, carrying transplanted NSCs either with or without CoPt NPs labelling (b or a, respectively). MRI of spinal cord slices showed regions of hypointense signal attributable to CoPt-labeled NSCs (b). Arrowheads indicate grafted CoPt-labeled NSCs which were represented by two dark spots in spinal cord slices (b). No hypointense regions were detected by MRI when similar numbers of unlabeled cells were implanted (a). Corresponding Hoechst 33342 labeling (c) and anti-nestin immuohistochemical staining (d) were carried out immediately after the MRI procedure on exactly the same spinal cord slices. CoPt-labeled NSCs still maintained multipotency after transplantation, which differentiated into astrocytes (e: Hoechst 33342, f: anti-nestin, g: anti-GFAP, h: merged) and neurons (i: Hoechst 33342, j: anti-Tuj1, k: anti-GFAP, l: merged) in the spinal cord slice. Bars = 10 μm.

slices, although magnetic nanoparticles might influence the differentiation of NSCs, as has been reported elsewhere.[20] The "graft-in-a-slice" paradigm offers a number of advantages as an *ex vivo* transplantation model which allows us to assess MRI of nanoparticle-labeled cells in a 3D environment, which could potentially mimic the *in vivo* condition of spinal cord transplantation. The cytoarchitectonic tissue organization is well preserved and spinal cord slices can be maintained in culture for several weeks. Moreover, slice cultures allow a number of procedures that are not presently feasible *in vivo* including tracking individual cells using time-lapse microscopy, immunological staining and high resolution MRI. These findings from this study therefore could potentially contribute toward our understanding of monitoring CoPt NP-labeled cells *in vivo* under a variety of transplantation conditions and over extended periods.

4 Conclusions

Here we established *in vitro* and *ex vivo* that the biology of NSCs is not altered by CoPt NP labeling. CoPt NP-loaded NSCs are detectable at low cell numbers invasively under MRI, in both 2D cell cultures and in 3D organotypic spinal cord slice models. The use of CoPt nanoparticles to label transplanted NSCs may help to identify the behaviours of the grafted stem cells post-transplantation, and therefore significantly reduce the animal numbers and refine the techniques required in the pre-clinical studies, and consequently may have significant impact on the delivery of NSCs in regenerative medicine.

Acknowledgements

Nguyen T. K. Thanh and Bing Song thank the Royal Society for their University Research Fellowships. Bing Song is supported by the European Research Council StG grant 243261. We thank Dr. Ioannis Lavdas for advice and help with surface coil MRI studies.

References

1 M. J. Hooshmand, C. J. Sontag, N. Uchida, S. Tamaki, A. J. Anderson and B. J. Cummings, *PLoS One*, 2009, **4**, e5871.
2 M. F. Rauch, S. R. Hynes, J. Bertram, A. Redmond, R. Robinson, C. Williams, H. Xu, J. A. Madri and E. B. Lavik, *Eur. J. Neurosci.*, 2009, **29**, 132–145.
3 S. Thuret, L. D. Moon and F. H. Gage, *Nat. Rev. Neurosci.*, 2006, **7**, 628–643.
4 W. J. Rogers, C. H. Meyer and C. M. Kramer, *Nat. Clin. Pract. Cardiovasc. Med.*, 2006, **3**, 554–562.
5 L. M. Parkes, R. Hodgson, T. Lu le, D. Tung le, I. Robinson, D. G. Fernig and N. T. K. Thanh, *Contrast Media Mol. Imaging*, 2008, **3**, 150–156.
6 K. O'Grady, *J. Phys. D: Appl. Phys.*, 2009, **42**, 220301.
7 F. H. Wang, I. H. Lee, N. Holmstrom, T. Yoshitake, D. K. Kim, M. Muhammed, J. Frisen, L. Olson, C. Spenger and J. Kehr1, *Nanotechnology*, 2006, **17**, 1911–1915.
8 M. Song, Y. G. Kim, Y. H. Kim, S. Ryu, I. C. Song, S. U. Kim and B. W. Yoon, *Neurosci. Res.*, 2009, **64**, 235–239.
9 L. T. Lu, L. D. Tung, I. Robinson, D. Ung, B. Tan, J. Long, A. I. Cooper, D. G. Fernig and N. T. K. Thanh, *J. Mater. Chem.*, 2008, **18**, 2453–2458.
10 T. L. Le, L. D. Tung, J. Long, D. G. Fernig and N. T. K. Thanh, *J. Mater. Chem.*, 2009, **19**, 6023–6028.
11 R. Guzman, N. Uchida, T. M. Bliss, D. He, K. K. Christopherson, D. Stellwagen, A. Capela, J. Greve, R. C. Malenka, M. E. Moseley, T. D. Palmer and G. K. Steinberg, *Proc. Natl. Acad. Sci. U. S. A.*, 2007, **104**, 10211–10216.
12 B. Bonnici and J. P. Kapfhammer, *Eur. J. Neurosci.*, 2008, **27**, 2483–2492.
13 H. Shichinohe, S. Kuroda, S. Tsuji, S. Yamaguchi, S. Yano, J. B. Lee, H. Kobayashi, S. Kikuchi, K. Hida and Y. Iwasaki, *Neurorehabilitation and Neural Repair*, 2008, **22**, 447–457.
14 X. T. Meng, D. Chen, Z. Y. Dong and J. M. Liu, *Cell Biol. Int.*, 2007, **31**, 691–698.
15 W. Kueng, E. Silber and U. Eppenberger, *Anal. Biochem.*, 1989, **182**, 16–19.
16 L. Stoppini, P. A. Buchs and D. Muller, *J. Neurosci. Methods*, 1991, **37**, 173–182.
17 M. Neri, C. Maderna, C. Cavazzin, V. Deidda-Vigoriti, L. S. Politi, G. Scotti, P. Marzola, A. Sbarbati, A. L. Vescovi and A. Gritti, *Stem Cells*, 2008, **26**, 505–516.
18 Y. Knobel, M. Glei, K. Osswald and B. L. Pool-Zobel, *Toxicol. in Vitro*, 2006, **20**, 793–800.
19 D. Ung, L. D. Tung, G. Caruntu, D. Delaportas, I. Alexandrou, I. A. Prior and N. T. K. Thanh, *CrystEngComm*, 2009, **11**, 1309–1316.
20 A. Focke, S. Schwarz, A. Foerschler, J. Scheibe, J. Milosevic, C. Zimmer and J. Schwarz, *Magn. Reson. Med.*, 2008, **60**, 1321–1328.

 This journal is © The Royal Society of Chemistry 2011